Article

Implementation of an Energy Management Strategy with Drivability Constraints for a Dual-Motor Electric Vehicle

Haiqing Wang and Hanfei Wu *

FEIT of University of Technology Sydney, Sydney, NSW 2007, Australia; Hq.wang.zoey@gmail.com

* Correspondence: Hanfei.Wu@student.uts.edu.au

check for updates

Abstract: This paper presents a real-time energy management strategy to distribute the power demand between two independent motors properly. Based on the characteristics of the novel transmission system, an enumeration-based searching approach is used to hunt for the optimal working points for both motors to maximize the overall efficiency. Like many energy management strategies, approaches that focus on reducing energy consumption can result in frequent gearshifts. To improve drivability and make a balance between energy consumption and gearshifts, a cost function is designed. To verify the effectiveness of the proposed method, a mathematical model is built, and the simulation results demonstrate the achieved improvements.

---

1. Introduction

As the energy resource shortage is becoming increasingly serious, the vehicle industry is facing an unprecedented challenge [1–3]. Due to the rising price of traditional energy sources such as fossil fuels and the penalty agreement on green gas emissions globally, the traditional transportation industry is transferring to electrical transport options which are more efficient in terms of energy usage and more environmentally friendly. As a consequence, researchers and manufacturers are paying more attention to hybrid electric vehicles (EVs) and pure electric vehicles which are more cost-effective, make cleaner usage of energy, and give better driving comfort [4]. However, the low energy-storage capacity of the batteries limits the driving distance significantly, leading to the unsuccessful popularization of EVs in the commercial market [5]. Therefore, measures should be taken in every possible way to optimize the usage of stored energy [6,7].

Transmission is fundamental to realize a high-efficiency electric powertrain with little compromise in driving ability [8,9]. Up to now, research has tended to focus on the application of multispeed transmission rather than single-speed transmission. Extensive research has shown that the motor size can be reduced by applying multispeed transmissions to electric vehicle platforms, as well as achieving the desired power by providing a wider speed range of usable torque and reducing energy consumption by gear-shifting [10]. In all current kinds of multispeed transmission, AMT stands out as a proper choice of electric vehicle transmission due to the advantages of the technique's maturity, reliable running performance, and good efficiency [11]. Besides, it also has a low manufacturing cost and compact size [12]. The disadvantages of this transmission system, such as vibration and torque interruption while shifting, cannot be ignored, as well as the clutch failures resulting from significant wear [13,14].

However, these drawbacks can be improved in electric vehicles because electric motors have a controllable actuating speed, which makes it possible to run a clutchless transmission system in electric vehicles to minimize the additional losses [11,15,16]. Moreover, to eliminate the torque interruption of AMT, a dual-motor platform is used to fill the torque hole during shifting with another motor [17–19].

The power distribution is important in energy management besides the structure of the powertrain [20]. Related research areas are developing fast in diverse ways. The rule-based control strategy is the most common and simplest control method. Its advantages are the high computing speed, simple architecture, and good control performance, such as shown in [21,22]. The fuzzy logic control strategy is good at balancing the efficiency of whole powertrain components, since this method can allow the possibility of imprecise measurements and uncertain changes between components [23,24]. A global optimization-based control strategy such as stochastic dynamic programming (SDP) uses an improved computing method, making the best decisions according to the results, which come from the former problems into the next situation until the end, such as in [25,26]. Model predictive control (MPC) incorporates the future driving load in the predictive model to manage the upcoming driving status [27]. The main weakness of these theories is that the optimal solution depends highly on pre-existing knowledge, so it is difficult to apply to real driving conditions that are full of uncertainty. The equivalent consumption minimization strategy (ECMS) transfers the electric energy consumption to fuel consumption by using an equivalent factor [28]. However, it cannot be used in the dual-motor input structure since the battery supporting both motors is working as the only power source without power transfer problems. To address this issue, a specific energy management strategy is designed using an enumeration algorithm.

It is worth noting that most studies in the energy management field have only focused on the optimization of energy consumption, while failing to address the drivability attributes. Excessive gear shifting [29] is one of the most typical problems encountered by energy management strategies, as achieving the best efficiency inherently requires frequent gear changes. To solve this problem, a specific shifting stability control approach is proposed. It employs a bump function to both control the minimum shifting frequency and reveal the relationship between the shifting frequency and the shifting cost penalty. As there are two parameters, namely the bump amplitude and bump duration in determining the cost function, an advanced optimization strategy which can solve the two-objective problem is adopted [30]. The proposed particle swarm optimization (PSO) multiobjective optimization method could generate a pair of desirable parameters according to specific driving conditions, thus achieving both low gear shift numbers and low energy consumption.

This paper proposes a real-time energy management strategy to improve the overall efficiency of a dual-motor transmission system. Since energy-oriented strategies often lead to frequent gearshifts, an optimization method based on PSO is adopted to filter undesirable gearshifts. The rest paper is organized as follows. In Section 2, the powertrain mathematical modeling and parameter selection of electric motors are introduced. Section 3 presents the designed energy management strategy and cost function for shift stability. Section 4 shows the simulation results of driving cycles. Conclusions are drawn in Section 5.

2. Powertrain Modeling

To maximize energy efficiency while meeting drivability requirements, clutchless dual-motor transmission is utilized. The structure of the transmission system is shown in Figure 1.

In the dual-input clutchless transmission system, EM1 and EM2 denote the first motor and the second motor respectively, and Dif. represents the differential mechanism. The red arrows illustrate the power flow provided by EM1 and the green arrows show the power flow by EM2. From the Figure 1, the first motor is connected to a multispeed transmission. Since electric motors are speed-controllable, gearshifts can be achieved without clutches. The combination of motor speed control and synchronizer actuation make it a cost-effective and efficient way to achieve the merits of multispeed transmission. In order to realize power-on shifting, the second motor helps compensate the torque hole during gearshifts. As the second motor drives the wheels using a fixed reduction ratio, the first and second motors can supplement each other to provide power in some driving conditions.
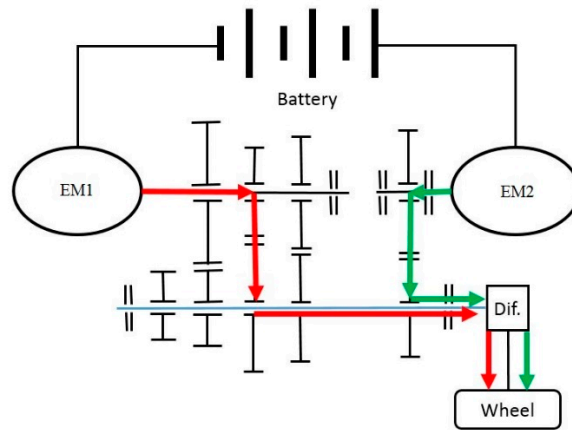
Figure 1. Dual-motor transmission.

The battery model based on the DC circuit is used for both motors in this study. This allows for direct model control through the input voltage, and the complexity inherent in power electronics is lost. The differential equation is calculated as:

$$L\dot{I} = K_e\dot{\theta} - RI + V \tag{1}$$

where L denotes the inductance, I denotes the line current, K_e is the electromagnetic field constant, R is the line resistance, and V is the voltage. The motor torque is calculated as:

$$T = K_T I \tag{2}$$

where K_T is the torque coefficient. The chief question that must first be considered about the motors is which of the two motors is the primary drive motor and how much power is required. Obviously, the use of multiple speed ratios is beneficial to improving the driving efficiency of the vehicle under a wider speed range, and thus EM1 should be considered the primary driving motor. The motor driving the fixed ratio, hereafter referred to as EM2, is required to provide additional driving power during certain periods of operation and provide high torque outputs for shifting. If a gear shift is undertaken whilst EM1 is driving the wheels at its peak output torque in any given speed, then the EM2 torque requirements can be defined and the peak power requirements of the motor established. The peak torque for EM2 that should be delivered during a generic up or down shift is defined, excluding any losses in the transmission, as:

$$T_2 = \frac{i_1 i_2}{i_3} T_1 \tag{3}$$

where i_1 is the gear ratio for multispeed transmission, i_2 is the counter shaft gear ratio, and i_3 is the fixed reduction gear ratio for the second motor, EM2. The speed range required for this torque delivery is defined as:

$$N_2 = \frac{i_3}{i_1 i_2} N_1 \tag{4}$$

Obviously, these two equations demonstrate that the speed and torque requirements for any particular gear shift produce identical peak power requirements to the primary driving motor. This is necessarily considered as overdesign of the motor as this power would only be required for the one to two seconds required for the gear shift. A balance must therefore be achieved through a review of the shifting patterns of the vehicle under a typical driving cycle. The motor efficiency maps are shown in Figure 2.
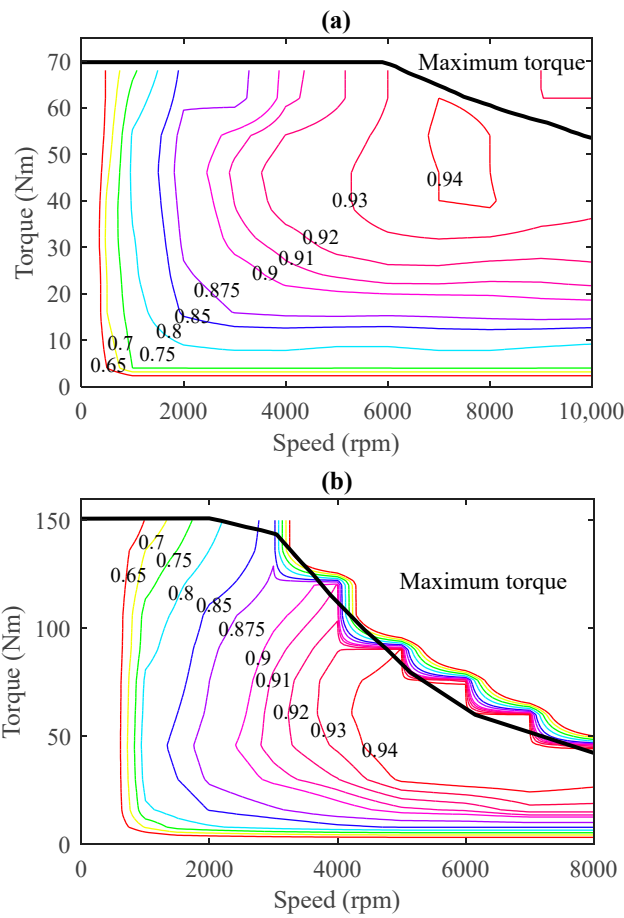
(a)

(b)

Figure 2. Motor efficiency maps.

The selected gear ratios are shown in Table 1.

Table 1. Gear ratios.

Symbol	Variable Name	Value
i_{c1}	Counter gear for motor 1	4.62
i_{c2}	Counter gear for motor 2	2.16
I_{g1}	Gear 1 for motor 1	3.46
i_{g2}	Gear 2 for motor 1	2.08
i_{g3}	Gear 3 for motor 1	1.32
i_2	Reduction gear for motor 2	3.46

These gear ratios are designed to cover most driving conditions. The first and second gear ratio of AMT is set to be relatively high to meet the requirements of urban driving conditions, where the vehicle speed is low and stops are frequent. By doing this, EM1 can work in a more efficient area by adjusting torque and speed through a large gear ratio. Then, the third gear ratio of AMT, as well as the fixed gear ratio of EM2, is designed to meet the requirements of mid-to-high-speed driving conditions, especially for traveling and highway cruising.

3. Energy Management Strategy

In order to maximize energy efficiency while meeting dynamic requirements, the energy management strategy plays an important role to distribute the power flow between two motors. Two motors should work in a supplementary way to achieve a desirable efficiency.

The output power is calculated as follows:

$$P_{out} = T_1 * \frac{\dot{\theta}_1}{\eta_1} + T_2 * \frac{\dot{\theta}_2}{\eta_2} \left(T_1 * \dot{\theta}_1 > 0 \& T_2 * \dot{\theta}_2 > 0 \right) \tag{5}$$

where η_1 is the efficiency of the first motor and η_2 is that of the second motor.

To optimize energy usage, both motors can work as a generator to charge the battery. The working conditions of regenerative braking is also included as well. Accordingly, the reusable power consumption is calculated as follows:

$$P_{in} = T_1 * \frac{\dot{\theta}_1}{\eta_1} + T_2 * \frac{\dot{\theta}_2}{\eta_2} \left(T_1 * \dot{\theta}_1 < 0 \& T_2 * \dot{\theta}_2 < 0 \right) \tag{6}$$

The overall power consumption is calculated as below:

$$P = P_{output} + P_{input} \tag{7}$$

In this equation, the variables are T_1, T_2, θ_1, and θ_2. However, they are not independent of each other.

As for the motor torques, the relation between two motors' can be described as

$$T_2 = \frac{J_{eq3} * \overline{\alpha_{Final}} + T_v - i_1 * \left(T_1 - J_{eq1} * \overline{\alpha_1} \right)}{i_2} + J_{eq2} * \overline{\alpha_2} \tag{8}$$

where J_{eq1} is the equivalent inertia for the first motor driveline, J_{eq2} is that for the second motor driveline, and J_{eq3} is that for the vehicle body. The $\overline{\alpha_{Final}}$, $\overline{\alpha_1}$, and $\overline{\alpha_2}$ are the demanded angular acceleration for the first motor, second motor, and final shaft, respectively. Once one of the motor torque values is decided upon, the other can be assigned. In this study, T_1 is used as the independent variable.

As to the speed, once the driving speed is given, the speeds of two motors are decided by the corresponding gear ratio. The equation can be expressed as below:

$$\dot{\theta}_{EM1} = \frac{\overline{v}}{R_w} \cdot i_1, \ \dot{\theta}_{EM2} = \frac{\overline{v}}{R_w} \cdot i_2 \tag{9}$$

Therefore, the independent variable in this system is the torque of EM1 and the corresponding gear ratio. As a result, the objective function is as below:

$$min \cdot P(T_1, i) \tag{10}$$

subject to

$$-\dot{\theta}_{1,max} \leq -\dot{\theta}_1 \leq \dot{\theta}_{1,max} \tag{11}$$

$$-T_{1,max}\left(\dot{\theta}_1\right) \leq T_{1,max} \leq T_{1,max}\left(\dot{\theta}_1\right) \tag{12}$$

$$-\dot{\theta}_{2,max} \leq -\dot{\theta}_2 \leq \dot{\theta}_{2,max} \tag{13}$$

$$-T_{2,max}\left(\dot{\theta}_2\right) \leq T_{2,max} \leq T_{2,max}\left(\dot{\theta}_2\right) \tag{14}$$

Since the battery is the only power source, there are no energy transfer issues. The enumerating method can reduce the computational burden while being as close as possible to the optimal solutions.

In the design space, the independent variable T_{M1} is discretized into a regular dense grid points of 2 Nm intervals. At these discretized points, the objective function value P is calculated under constraints. The optimal points with minimum objective values will be chosen as the final results after excluding the unfeasible points. Figure 3 shows the plots of the objective function; from this, it can be seen that the trajectory of the optimal solutions would be adjusted under different driving conditions.
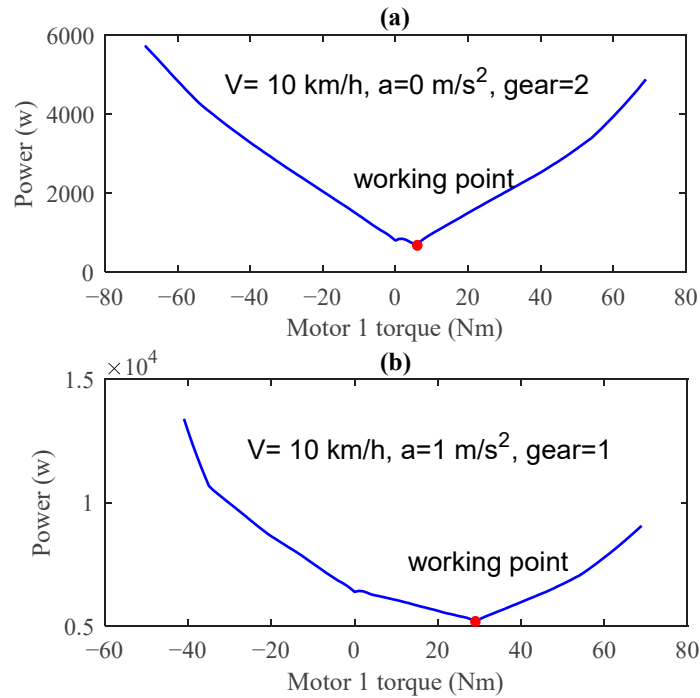
Figure 3. Objective function value of different driving conditions.

4. Shifting Stability

The energy management strategy can provide optimal power distribution between two motors, but it can also lead to frequent gear-shifting. To avoid this problem, a cost function is used in the proposed energy management strategy to improve shift stability. It is defined as follows:

$$f_{cost} = A * e^{-\frac{1}{1-x^2}}$$

(15)

The bump function is introduced as a penalty to solve the problem of frequent gearshifts. As shown in Figure 4, the penalty will start from a large value in the early period and then decrease smoothly but rapidly to zero.
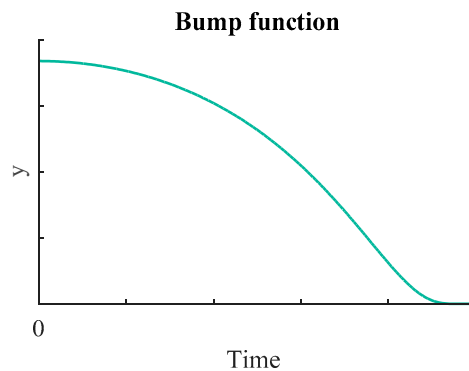

Figure 4. Feature of the bump function.

Figure 5 shows the schematic diagram of the designed cost function, where the solid lines denote the power consumption for each gear. Since the power consumptions of different gear states are not the same, the optimal gear is decided by searching for the gear ratio with minimum power consumption. Based on this, the gear will change with the lowest curves to save energy, which results in a short shifting duration. With the designed cost function, every time gear-shifting is completed, the power consumption of the current gear will keep its value, but additional penalty values will be imposed on the rest of the gears. As shown in Figure 5, the working gear changes from the blue line to the green line in the beginning, so that a penalty will be imposed on the nonworking gear due to the cost function. Thus, the shifting duration last for a longer period when searching for minimum power consumption and frequency of gearshifts is significantly reduced.
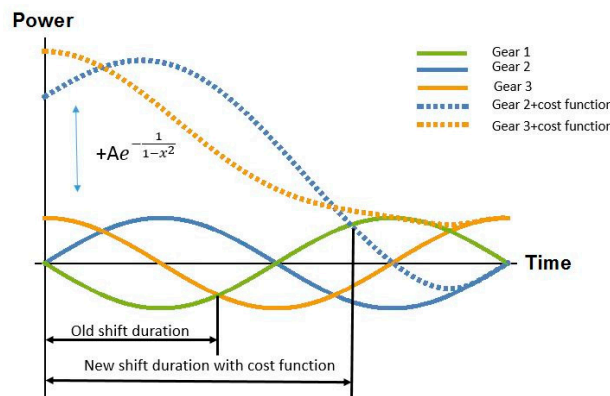

Figure 5. The schematic diagram of the designed cost function.

Considering the shifting stability, the objective function to be minimized in the energy management strategy will be defined as

$$P_{sub\_opt} = P + f_{cost} \tag{16}$$

However, since the gear-shifting directed by the energy management strategy aims at achieving high energy efficiency, the reduction of gear changes will lead to an increase in power consumption. To filter out unnecessary shifts while minimizing the extra energy consumption, the coefficients of the cost function is the key. In order to make a balance between energy consumption and gearshifts, the optimization approach based on particle swarm optimization is used to optimize the corresponding coefficients.

The PSO algorithm is a heuristic optimization algorithm that simulates the random distribution and instinct behavior of creatures, which are called particles. Particles interact with each other and move as a group, affecting the overall speed and location of all groups. The key element of PSO is the speed and position of swarms, which are respectively defined as follows:

$$V_{id}^{k+1} = \omega V_{id}^{k} + c_1 r_1 \left(P_{id}^{k} - X_{id}^{k} \right) + c_2 r_2 \left(P_{id}^{k} - X_{id}^{k} \right) \tag{17}$$

$$X_{id}^{k+1} = X_{id}^{k} + V_{id}^{k+1} \tag{18}$$

where ω is the inertial weight, k is the current number of iterations, V_{id} is the swarm speed, X_i is the fitness value, c_1 and c_2 are the non-negative constants called the acceleration factors, and r_1 and r_2 are random numbers between 0 and 1. The control configuration is shown in Figure 6.
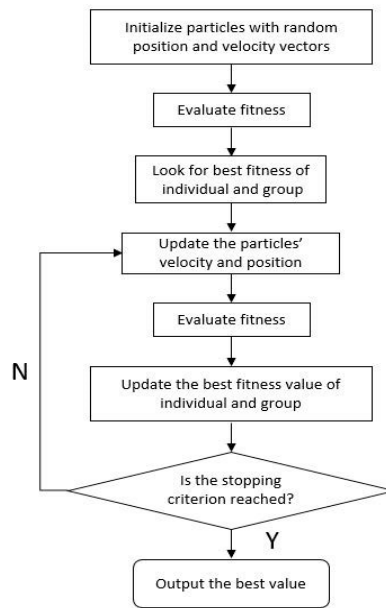
Figure 6. Multiobjective optimization control configuration.

In the PSO multiobjective optimization, the functions to be minimized are as follows:

$$f_1 = minP(T_1, i) + A * e^{-\frac{1}{1-x^2}} \tag{19}$$

$$f_2 = min \sum Gearshifts \tag{20}$$

Because f_1 and f_2 are not on the same order of magnitude, the values are normalized as below:

$$f'_{1k} = \frac{f_{1k}}{\overline{f_1}} \tag{21}$$

$$f'_{2k} = \frac{f_{2k}}{\overline{f_2}} \tag{22}$$

where f_{1k} denotes the value for the kth generation and $\overline{f_1}$ denotes the average value.

It worth noting that the PSO optimization is used to determine the coefficients of the cost function offline. The optimization results will be used in the online power-sharing strategy to help calculate the penalty instantaneously.

5. Performance Evaluation

5.1. Power-Sharing Strategy Evaluation

In order to demonstrate the effectiveness of the proposed power-sharing strategy, the LA92 driving cycle is adopted. The total distance of the LA92 cycle is 15.8 km, traveled in 1435 s. It is a representation of urban driving patterns for light-duty vehicles.

For comparison, different fixed power distribution strategies are investigated. Figure 7 shows the energy consumption comparisons.
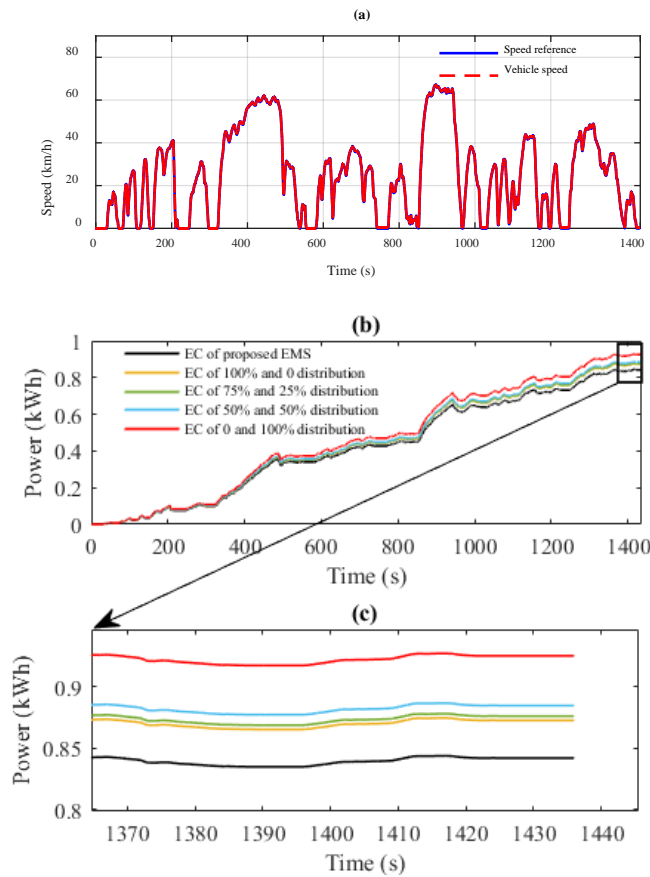
Figure 7. Energy consumption comparisons.

Figure 7a shows that there are many starts and stops along the LA92 driving cycle, which are shown in the form of speed peaks. From the speed file, the proposed energy management strategy can direct the vehicle to follow the target speed accurately. In Figure 7b, fixed distribution strategies are used to make a comparison. The trajectory of energy consumptions is not monotonically increasing because the motors can work as a generator in braking. The results show that the designed energy management strategy achieves the highest efficiency, where two motors work easily in their high-efficiency region with proper power distribution. Two motors can work in a supplementary way to provide power. The fixed distributions limit the possibility of optimal solutions. Two motors can hardly achieve their high-efficiency region simultaneously due to distribution constraints. The detailed energy consumption are shown in Table 2.

Table 2. Energy consumption comparison.

LA92	Energy Consumption	Extra EC
Proposed strategy	0.8418 kWh	
Motor 1 (100%); Motor 2 (0%)	0.8726 kWh	3.66%
Motor 1 (75%); Motor 2 (25%)	0.8761 kWh	4.07%
Motor 1 (50%); Motor 2 (50%)	0.8847 kWh	5.10%
Motor 1 (0%); Motor 2 (100%)	0.9252 kWh	9.91%

It is worth noting that when the first motor has the higher distribution weight, it confers higher efficiency. As shown in Table 2, the distribution of 100% of work done by motor 1 and 0% by motor 2 stands out in the fixed distribution strategies, followed by that with 75% of work done by motor 1 and 25% by motor 2, then that with 50% of work done by motor 1 and 50% by motor 2, and finally,

that in which only motor 2 is working. This is because of the advantage of multispeed transmission. Since motor 1 is connected to a multispeed transmission, the energy efficiency can be improved through gear changes, especially in complex and changeable driving conditions. On the other hand, when it comes to stable driving conditions such as cruising, the energy efficiency will increase with the weight of the second motor. This is because the second motor works better in low-torque high-speed conditions. So, for different driving situations, the designed power-sharing strategy can always find a decent power distribution ratio to achieve a higher energy efficiency.

5.2. Drivability Evaluation

Figure 8 shows the corresponding shifting performance and motor speeds. The upper figure represents the gear shift numbers while the lower figure shows the motor rotational speed along with time.
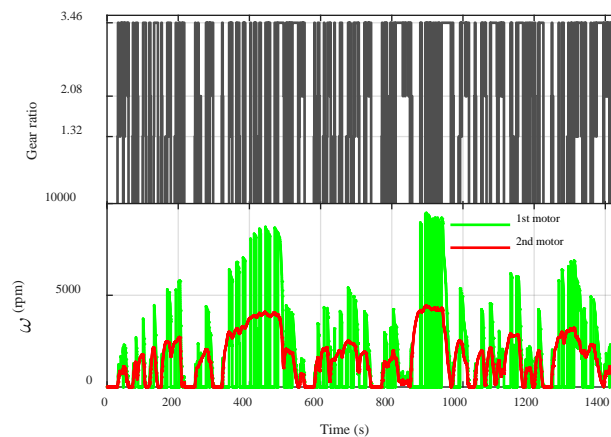

Figure 8. Gear shifting with the power-sharing strategy.

From Figure 8, it can be seen in the upper figure that in order to achieve high overall efficiency, the gear kept changing throughout the whole process, which introduced energy losses and reduced comfort of the driving experience. In the lower figure of Figure 8, the motor speed figure shows that both motors help to provide power with the proposed strategy. When the vehicle speed is lower than 40 km/h, the first motor works as the main power source. The motor speed is high to achieve high efficiency, according to the motor efficiency map. Besides, the multispeed transmission can provide high launching torque without compromising efficiency at high operating speed. When the vehicle speed is beyond 40 km/h, the second motor will help to provide power with low torque and high speed to guarantee the optimal efficiency.

The motor speed figure demonstrates that motor 1 mainly works when the vehicle speed is low while the motor speed is high to achieve high efficiency. In low-speed conditions, motor 1 works together with AMT to achieve high efficiency, because AMT provides high starting torque without compromising the efficiency at high operating speed. When the vehicle speed is above 40 km/h, motor 2 will take over to provide power due to the design of the fixed gear ratio for motor 2.

To alleviate the frequent gearshifts, the optimized cost function is adopted, and the improved shifting performance is shown in Figure 9.
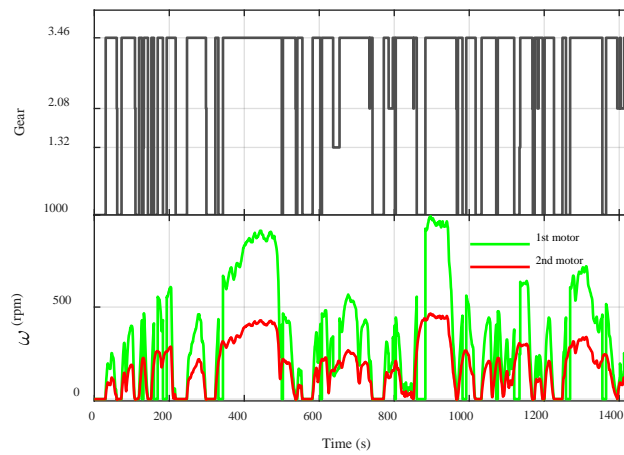
Figure 9. Gear shifting with the modified power-sharing strategy.

Compared to Figure 8, the gear-shifting frequency has been greatly reduced. The motor speed file shows that the performance of the first motor works in a steady and continuous way with less frequent starting and stopping.

Table 3 explicates the drivability improvement and compares the suboptimality of energy consumption. The energy-oriented power-sharing strategy causes 392 shifts in the LA92 driving cycle, with one shift every 4 s on average. Moreover, many gear states last for less than 2 seconds. In comparison, with the help of shifting stability control, the number of shifts reduces to 75, with one shift every 19 s on average. The shift duration is increased by almost 5 times, and the number of shifts lasting for too short a time are significantly reduced. However, the reduction of gear shifts gives rise to suboptimal energy consumption, which rises from 0.8418 kWh to 0.8519 kWh.

Table 3. Drivability improvement and energy consumption.

LA92	Before	After
Gear shifts	392	75
Average shifting duration	4 s	19 s
Shifts lasting less than 2 s	254	22
Energy consumption	0.8418 kWh	0.8519 kWh

Figure 10 shows the power consumption under shift stability control. It can be seen that the significant reduction of gearshifts only leads to 1.2% extra power consumption.
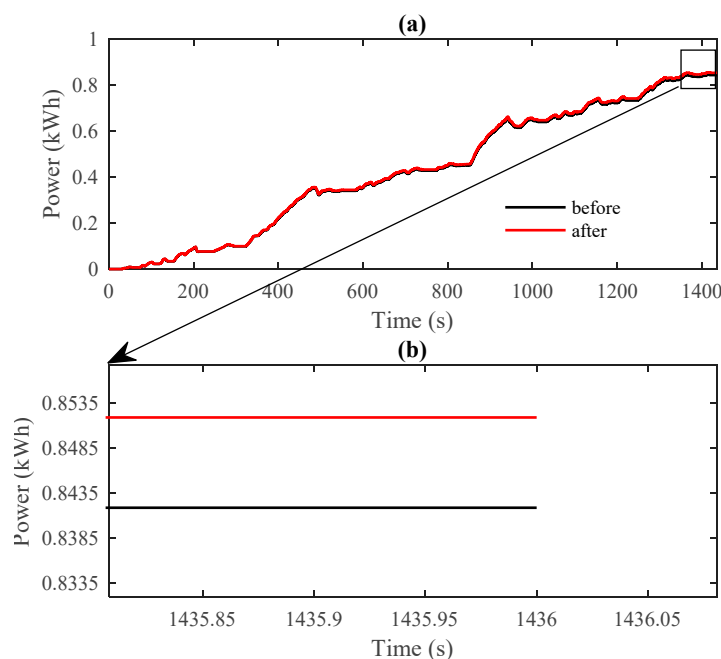
Figure 10. Power consumption with and without shift stability control.

6. Conclusions

This paper presents a real-time power-sharing strategy with the corresponding shifting stability control algorithm for a new dual-input clutchless transmission system. The power-sharing strategy could adequately distribute the power demand to the motors in the system, achieving a relatively high overall efficiency. To solve the inherent frequent shifting problem, a decent cost function is designed, which considers both the minimum gear change duration and the interval between two adjacent gear shifts. To optimize the overall efficiency and the gear shift frequency, a multiobjective optimization method is proposed, which decides both the amplitude and the duration of the cost function. A detailed mathematic model has been built and the improvements achieved by the proposed system have been verified.

Author Contributions: Conceptualization, H.W. (Hanfei Wu); Data curation, H.W. (Haiqing Wang); Methodology, H.W. (Haiqing Wang); Writing—original draft, H.W. (Haiqing Wang); Writing—review & editing, H.W. (Hanfei Wu).

Conflicts of Interest: The authors declare no conflict of interest.

References

1. Apostolaki-Iosifidou, E.; Codani, P.; Kempton, W. Measurement of power loss during electric vehicle charging and discharging. *Energy* **2017**, *127*, 730–742. [CrossRef]
2. Zhang, J.; Li, Y.; Lv, C.; Yuan, Y. New regenerative braking control strategy for rear-driven electrified minivans. *Energy Convers. Manag.* **2014**, *82*, 135–145.
3. Fajri, P.; Lee, S.; Prabhala, V.A.K.; Ferdowsi, M. Modeling and integration of electric vehicle regenerative and friction braking for motor/dynamometer Test Bench Emulation. *IEEE Trans. Veh. Technol.* **2016**, *65*, 4264–4273. [CrossRef]
4. Cipek, M.; Pavković, D.; Petrić, J. A control-oriented simulation model of a power-split hybrid electric vehicle. *Appl. Energy* **2013**, *101*, 121–133. [CrossRef]
5. Nykvist, B.; Nilsson, M. Rapidly falling costs of battery packs for electric vehicles. *Nat. Clim. Chang.* **2015**, *5*, 329–332. [CrossRef]

6.   Sabri, M.; Danapalasingam, K.; Rahmat, M. A review on hybrid electric vehicles architecture and energy management strategies. *Renew. Sustain. Energy Rev.* **2016**, *53*, 1433–1442. [CrossRef]

7.   Onori, S.; Serrao, L.; Rizzoni, G. *Hybrid Electric Vehicles: Energy Management Strategies*; Springer-Verlag London: London, UK, 2016.

8.   Lu, Z.; Song, J.; Fang, S.; Li, F.; Yu, L. Shifting Control of Uninterrupted Multi-Speed Transmission Used in Electric Vehicle. In Proceedings of the ASME 2018 International Design Engineering Technical Conferences and Computers and Information in Engineering Conference, Quebec, QC, Canada, 26–29 August 2018; p. V003T01A039.

9.   Liang, J.; Zhang, Y.; Zhong, J.-H.; Yang, H. A novel multi-segment feature fusion based fault classification approach for rotating machinery. *Mech. Syst. Signal Process.* **2019**, *122*, 19–41. [CrossRef]

10. He, H.; Liu, Z.; Zhu, L.; Liu, X. Dynamic coordinated shifting control of automated mechanical transmissions without a clutch in a plug-in hybrid electric vehicle. *Energies* **2012**, *5*, 3094–3109. [CrossRef]

11. Liang, J.; Yang, H.; Wu, J.; Zhang, N.; Walker, P.D. Power-on shifting in dual input clutchless power-shifting transmission for electric vehicles. *Mech. Mach. Theory* **2018**, *121*, 487–501. [CrossRef]

12. Gao, B.; Liang, Q.; Xiang, Y.; Guo, L.; Chen, H. Gear ratio optimization and shift control of 2-speed I-AMT in electric vehicle. *Mech. Syst. Signal Process.* **2015**, *50*, 615–631. [CrossRef]

13. Yang, W.; Liang, J.; Yang, J.; Zhang, N. Optimal control of a novel uninterrupted multi-speed transmission for hybrid electricmining trucks. *Proc. Inst. Mech. Eng. Part D J. Autom. Eng.* **2019**. [CrossRef]

14. Yan, Z.; Yan, F.; Liang, J.; Duan, Y. Detailed modeling and experimental assessments of automotive dry clutch engagement. *IEEE Access* **2019**. [CrossRef]

15. Tseng, C.-Y.; Yu, C.-H. Advanced shifting control of synchronizer mechanisms for clutchless automatic manual transmission in an electric vehicle. *Mech. Mach. Theory* **2015**, *84*, 37–56. [CrossRef]

16. Liang, J.; Yang, H.; Wu, J.; Zhang, N.; Walker, P.D. Shifting and power sharing control of a novel dual input clutchless transmission for electric vehicles. *Mech. Syst. Signal Process.* **2018**, *104*, 725–743. [CrossRef]

17. Holdstock, T.; Sorniotti, A.; Everitt, M.; Fracchia, M.; Bologna, S.; Bertolotto, S. Energy consumption analysis of a novel four-speed dual motor drivetrain for electric vehicles. In Proceedings of the 2012 IEEE Vehicle Power and Propulsion Conference, Seoul, Korea, 9–12 October 2012; pp. 295–300.

18. Zhang, S.; Xiong, R.; Zhang, C.; Sun, F. An optimal structure selection and parameter design approach for a dual-motor-driven system used in an electric bus. *Energy* **2016**, *96*, 437–448. [CrossRef]

19. Liang, J.; Walker, P.D.; Ruan, J.; Yang, H.; Wu, J.; Zhang, N. Gearshift and brake distribution control for regenerative braking in electric vehicles with dual clutch transmission. *Mech. Mach. Theory* **2019**, *133*, 1–22. [CrossRef]

20. Wu, H.; Walker, P.; Wu, J.; Liang, J.; Ruan, J.; Zhang, N. Energy management and shifting stability control for a novel dual input clutchless transmission system. *Mech. Mach. Theory* **2019**, *135*, 298–321. [CrossRef]

21. Wirasingha, S.G.; Emadi, A. Classification and review of control strategies for plug-in hybrid electric vehicles. *IEEE Trans. Veh. Technol.* **2011**, *60*, 111–122. [CrossRef]

22. Peng, J.; He, H.; Xiong, R. Rule based energy management strategy for a series–parallel plug-in hybrid electric bus optimized by dynamic programming. *Appl. Energy* **2017**, *185*, 1633–1643. [CrossRef]

23. Serrao, L.; Onori, S.; Rizzoni, G. A comparative analysis of energy management strategies for hybrid electric vehicles. *J. Dyn. Syst. Meas. Control* **2011**, *133*, 031012. [CrossRef]

24. Yin, H.; Zhou, W.; Li, M.; Ma, C.; Zhao, C. An adaptive fuzzy logic-based energy management strategy on battery/ultracapacitor hybrid electric vehicles. *IEEE Trans. Transp. Electrif* **2016**, *2*, 300–311. [CrossRef]

25. Romaus, C.; Gathmann, K.; Böcker, J. Optimal energy management for a hybrid energy storage system for electric vehicles based on stochastic dynamic programming. In Proceedings of the Vehicle Power and Propulsion Conference (VPPC), Lille, France, 1–3 September 2010; pp. 1–6.

26. Zhang, S.; Xiong, R. Adaptive energy management of a plug-in hybrid electric vehicle based on driving pattern recognition and dynamic programming. *Appl. Energy* **2015**, *155*, 68–78.

27. Valenzuela, G.; Kawabe, T.; Mukai, M. Nonlinear model predictive control of battery electric vehicle with slope information. In Proceedings of the 2014 IEEE International Electric Vehicle Conference (IEVC), Florence, Italy, 17–19 December 2014; pp. 1–5.

28. Serrao, L.; Onori, S.; Rizzoni, G. ECMS as a realization of Pontryagin's minimum principle for HEV control. In Proceedings of the 2009 American control conference, St. Louis, MO, USA, 10–12 June 2009; pp. 3964–3969.

29. Miro-Padovani, T.; Colin, G.; Ketfi-Chérif, A.; Chamaillard, Y. Implementation of an energy management strategy for hybrid electric vehicles including drivability constraints. *IEEE Trans. Veh. Technol.* **2016**, *65*, 5918–5929. [CrossRef]
30. Yu, W.; Li, B.; Jia, H.; Zhang, M.; Wang, D. Application of multi-objective genetic algorithm to optimize energy efficiency and thermal comfort in building design. *Energy Build.* **2015**, *88*, 135–143. [CrossRef]